

Influence of shape and perimeter length on induced color contrast

Qasim Zaidi, Billibon Yoshimi, and John Flannigan

Department of Psychology, Columbia University, New York, New York, 10027

Received February 11, 1991; revised manuscript received June 24, 1991; accepted June 25, 1991

The magnitude of induced color contrast was measured for tests whose areas, perimeter lengths, and shapes were independently varied. Test shapes were smoothly contoured, multiple-lobed figures generated from unitary Fourier shape descriptors. The shapes had from 3 to 40 lobes and were equal in area to a disk of diameter 2 deg, with perimeter lengths of 1.25, 1.75, 2.25, and 2.75 times the circumference of a 2-deg disk. The surround was a 5-deg disk. The surround was modulated sinusoidally along one of the three cardinal directions of color space around an equal-energy white of 50 cd/m². The observer nulled the modulation induced into the test by adjusting the amplitude of real modulation in the test. The amplitude of nulling modulation was the measure of induction. The main result was that the amount of induction was similar for all tests of equal area irrespective of the shape or the length of perimeter.

INTRODUCTION

Different objects in the world have different spectral reflectances. An observer is able to segment objects in a visual scene because different reflectances correlate with the phenomenal experience of different colors. In addition, different parts of a three-dimensional object reflect different amounts of ambient light to the eye of an observer. This phenomenon enables an observer to infer the shape of an object from the relative brightness of different parts in the two-dimensional retinal image. The computation of the color of different parts of a visual image thus serves a number of important functions. It is known that this computation includes serial and lateral interactions of the photoreceptor signals evoked by the incident optic array.¹ It has also been shown that perceived color is not independent of factors such as perceived depth and transparency.^{2,3}

In general it is difficult to measure absolute aspects of perceived colors quantitatively in a manner conducive to relating these measurements to properties of theoretical processes. However, the effects of some of the processes involved in the computation of perceived color can be isolated and estimated by the measurement of the change in the color of a test patch that is due to induced contrast from surrounding colors.⁴ If the color of the surround is modulated periodically in time, the color of the test also appears to modulate in time. If the induced modulation can be nulled by the addition of real modulation to the test field, then the nulling modulation can be used as a precise measure of the induced effect. This method was used by Krauskopf *et al.*⁵ to show that the induced modulation in the test could be nulled by a modulation of the test colors along the same color line as the surround modulation and in roughly the same phase. The apparent color of a patch was thus changed by a surrounding color in the direction complementary to the inducing color. The nulling method requires the observer only to signal the absence or presence of modulation without extracting any subjective qualities of the test. This is a psychophysical procedure

that meets the requirements of Brindley's class A⁶ experiments. The following assumption can be used to link the psychophysical nulling measurements to the response of neural mechanisms:

If the visual appearance of a test field corresponds to the activity of at least some of the neural mechanisms whose receptive fields cover the retinal coordinates of the test, then at the null setting, despite there being real temporal modulation of the color of the test, the response of these neural mechanisms must be below perceptual threshold at some stage of the visual system and also at subsequent stages.

The results presented by Krauskopf *et al.*⁵ show that, at some stage of the visual system, the mechanisms excited by the surround alter the response of the neural mechanisms responsible for the appearance of the test patch. The nulling procedure can thus be used to estimate properties of the lateral interactions that affect the appearance of colors.

Results of experimental studies have led to a few qualitative generalizations about the effects of size of tests and surrounds and of the distance between them, but critical tests of the properties of the lateral interactions underlying color induction remain to be done. In part, the problem is that only a small number of spatial configurations have been tried. Studies that have varied the spatial configuration of test and inducing fields have generally used circular center-surround configurations or rectangular tests flanked by rectangular surrounds. The neural mechanisms responsible for color induction have also not been identified with any certainty. Despite these limitations, a number of models for the computation of brightness and color, incorporating lateral interactions, have been proposed.⁷⁻¹⁰ These models can be viewed as algorithmic embodiments of the notion that two types of process mediate induced color contrast: those that enhance contrast across boundaries and those that integrate

within closed boundaries to give a uniform appearance. Thus, fitting these models to quantitative data may make it possible to estimate the parameters of the two processes. However, as we discuss below, models of this class need further mathematical development before they can be useful for quantitative work. Yund and Armington¹¹ have provided an assumption that can be used to simplify the predictions made by elemental models. They assume that, in a display consisting of uniformly colored patches with sharp edges, the most important lateral interactions are localized at the edges. That is, in the computation of color at any point, it is only the position of edges with respect to the point that is important, with the effect of edges further away being weighted less. For a spatial configuration consisting of a circular test of radius R_T , surrounded by a concentric annulus of outer radius R_S , the magnitude of induced contrast should be proportional to

$$\frac{1}{R_T} - \frac{1}{R_S}. \quad (1)$$

An alternative conceptual approach to perceived color is Helson's adaptation level theory,¹² which suggests that the color of any point in a display is computed relative to an adaptation color that is to be regarded as the weighted mean of all parts of the visual scene. Helson's theory does not specify how the adaptation level is to be calculated for any specific stimulus configuration. For a center-surround arrangement, Yund and Armington¹¹ suggest that the induced effect should be proportional to the log of the ratio of the area of the surround to the area of the center:

$$\log\left(\frac{R_S^2 - R_T^2}{R_T^2}\right). \quad (2)$$

Yund and Armington¹¹ measured induced contrast in a large number of circular center-surround configurations. Their data ruled out a number of other models but were consistent with both formulas (1) and (2). As they point out, the predictions of formulas (1) and (2) are highly correlated for circular center-surround configurations, so such configurations cannot be used to distinguish between the two models.

The motivation behind this study was to learn more about the spatial nature of induced contrast by a separation of the effects of area, shape, and perimeter on the change in perceived color of a test patch. The test patches were multiple-lobed shapes like those in Fig. 1. The area, the number of lobes, and the lengths of the perimeters of these shapes were varied independently. By varying the number of lobes and the length of the perimeter, we varied the average distance from the edge to the center while keeping the area constant and thus providing a means of uncorrelating the predictions of the two models in formulas (1) and (2). There was an additional reason to vary the length of the perimeter. A sharp edge between a light and a dark region is an effective stimulus for many types of neuron in the visual system. A longer perimeter may excite more of these cells. However, little is known about the manner in which the outputs of neurons are combined to give a percept. It is unlikely that the outputs of neurons at any stage are just summed. Some models

postulate that the output of each V1 cortical neuron is normalized by the total output of neurons of different receptive field sizes and orientations.¹³ Estimates of the effect of length of perimeter on the magnitude of contrast induced into tests of equal area may be useful in understanding the pooling process. Similarly, little is known about the presumed syncytium that fills in the color within closed boundaries. The set of test shapes used in this study included subsets with equal area and perimeter length but a different number of lobes. Estimates of the effect of shape on induced contrast may provide useful information about the diffusion or spatial integration stages.

METHOD

Test Stimuli

A center-surround arrangement was used for studying induced color contrast. The novel feature of this study was the shape of the tests shown in Fig. 1, with the number of lobes being 3, 4, 5, 6, 7, 8, 9, 10, 20, or 40. The area of each test was equal to the area of a circle of radius 1 deg, i.e., equal to Π deg². The length of the perimeter of a test was 2.5Π , 3.5Π , 4.5Π , or 5.5Π deg. The test field was surrounded by a disk with an outer diameter of 5 deg.

The purposes of this experiment required tests whose shapes, areas, and perimeters could be varied independently. In addition it was considered desirable to use shapes with smooth contours and without sharp corners. The analytic expression for Fourier descriptors provided by Zahn and Roskies¹⁴ proved to be suitable for generating the test shapes. Equations (3) and (4) give the position (X, Y) on the curve as a function of the perimeter l :

$$X(l) = X_0 + \frac{L}{2\Pi} \int_0^l \cos\left[-t + \mu_0 + d_0 + \sum_{n=1}^{\infty} A_n \cos(nt - a_n)\right] dt, \quad (3)$$

	Perimeter Length (deg)			
	2.5Π	3.5Π	4.5Π	5.5Π
3				
4				
5				
6				
7				
8				
9				
10				
20				
40				

Fig. 1. Unitary Fourier descriptors of equal area, calculated from Eqs. (3) and (4), used as test stimuli in the experiment.

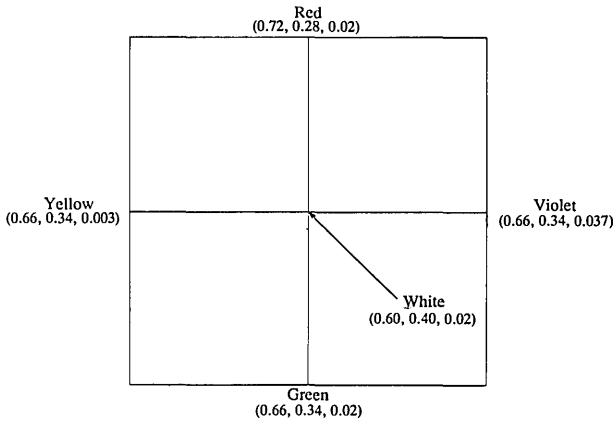


Fig. 2. Isoluminant lines of chromatic modulation used in the induction experiment are shown as the axes of a plane. Triplets in parentheses correspond to (L, M, S) coordinates of these lights in the MacLeod-Boynton¹⁷ chromaticity diagram.

$$Y(l) = Y_0 + \frac{L}{2\pi} \int_0^l \sin[-t + \mu_0 + d_0 + \sum_{n=1}^{\infty} A_n \cos(nt - \alpha_n)] dt. \quad (4)$$

X_0 and Y_0 are the starting X and Y locations, respectively. L is the total perimeter length. l varies from 0 to L . t is the perimeter parameter. μ_0 is the initial phase of the descriptor. d_0 is the initial direction. A_n is the magnitude of the n th-power descriptor. α_n is the phase of the n th power descriptor.

These equations can generate a large variety of closed contours with only a limited number of parameters. Each term in the equation has a parameter that is directly related to some aspect of the shape of the descriptor. For example, when A_n is nonzero for only one value of n , then the generated shape has n lobes. All the shapes in Fig. 1 are examples of such unitary descriptors. Fourier descriptors are rotationally invariant; for a unitary descriptor, the orientation depends on the starting location (X_0, Y_0). The total length of the perimeter is easily specified since the descriptor is generated as a function of its perimeter L . Intuitively, for a unitary descriptor of n lobes, L depends on the magnitude of A_n . When area is kept constant, the perimeter length is increased if one makes the lobes more distinct. The function for the area of unitary descriptors was calculated from Eq. (6) below. Because the derivatives of both $X(l)$ and $Y(l)$ with respect to l exist, Green's theorem¹⁵ was used to simplify the expression for the area enclosed by a closed curve:

$$\text{Area} = \int XdY = \int_{l=0}^{l=L} X(l) \times Y'(l) dl. \quad (5)$$

For any choice of parameters, Eq. (6) was used to compute the area:

$$\begin{aligned} \text{Area} = & \int_{l=0}^{l=L} \frac{L}{2\pi} \left\{ \int_{t=0}^{t=2\pi/L} \sin[-t + \mu_0 + d_0 + \sum_{n=1}^{\infty} A_n \cos(nt - \alpha_n)] dt \right\} \cos\left[\frac{-2\pi l}{L} + \mu_0 + d_0 + \sum_{n=1}^{\infty} A_n \cos(nt - \alpha_n)\right] dl. \quad (6) \end{aligned}$$

Modulation Colors

Induction was measured along the three cardinal directions of color space.¹⁶ The plane formed by the two chromatic directions is shown in Fig. 2. The origin and end points of the plane are described in approximate color names and in long-wavelength-sensitive (L), medium-wavelength-sensitive (M), and short-wavelength-sensitive (S) cone excitations¹⁸ with the use of the chromaticity coordinates of the MacLeod-Boynton¹⁷ diagram. The center of the plane was metameric to white at 50 cd/m². The third direction was the achromatic light-dark axis along which the luminance of the white point was modulated from 0 to 100 cd/m². Along the light-dark axis, the excitation of the three cone types was modulated proportionally. Along the green-red axis, the excitation of L and M cones changed in equal and opposite amounts to keep their sum constant, and the excitation of S cones was constant. Along the yellow-violet axis, only the excitation of the S cones changed. The color names are to be used solely as mnemonics; the appearance of the lights on the screen was more desaturated than suggested by the color names.

Measurement Procedure

The modulation-nulling technique introduced by Krauskopf *et al.*⁵ was used to measure the amount of induction within the test shape that was surrounded by a disk with an outer diameter of 5 deg. As is shown in Fig. 3, the color of the surrounding field was modulated sinusoidally at 1 Hz around the midwhite point along one of the three cardinal directions. The modulation of the surround induced a counterphase modulation into the central test. The observer adjusted the amplitude of real modulation inside the test along the same color line to null the induced modulation. The amplitude of nulling modu-

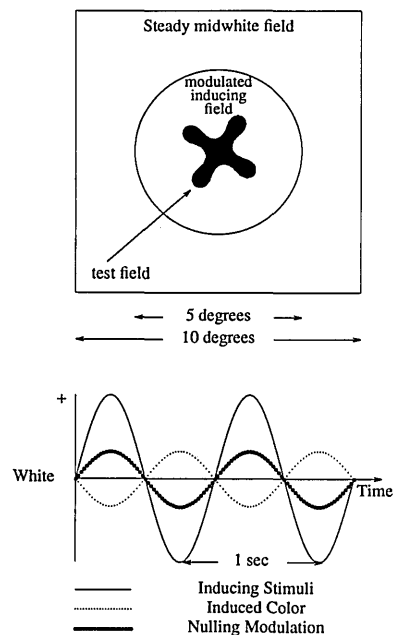


Fig. 3. Basic measurement technique. The top panel shows the spatial configuration of the inducing and test stimuli. In the bottom panel the solid curve depicts the variation in time of the color of the inducing field. The fine dotted curve depicts the modulated appearance of the test field when it is, in fact, not modulated. The curve consisting of larger filled circles depicts the real modulation of the test required to make it appear steady.

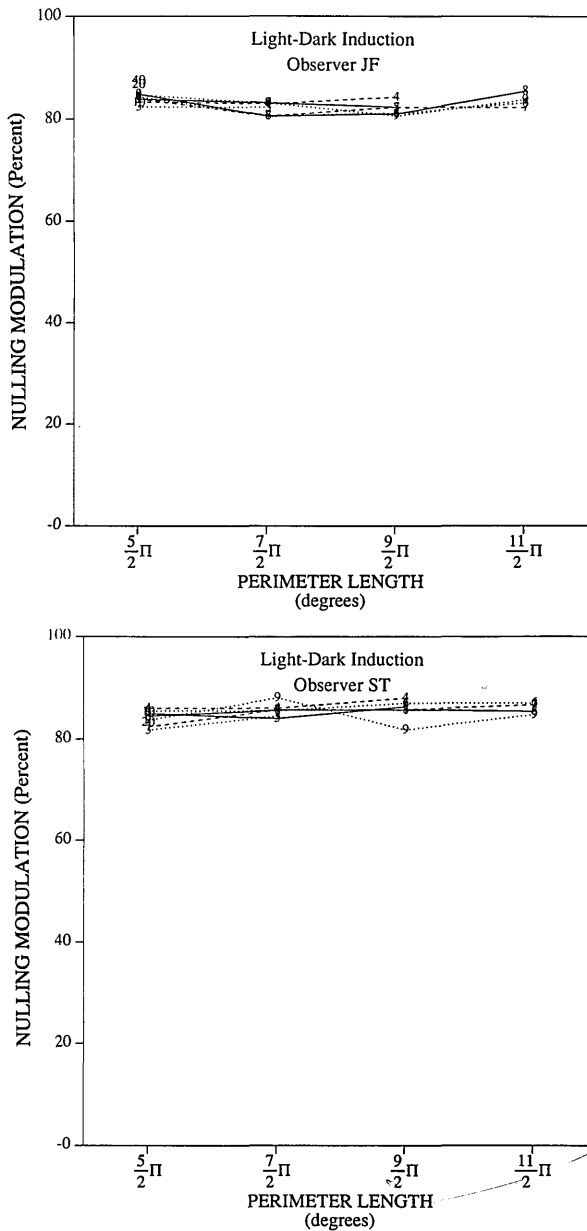


Fig. 4. Amplitude of nulling modulation in the light-dark direction expressed as a percentage of inducing modulation versus the length of the perimeter of the test. Each test stimulus is represented by a number indicating the number of lobes that range from 3 to 40. Curves connect nulling amplitudes for tests of the same number of lobes.

lation was used as the estimate of the magnitude of induced contrast.

Equipment and Stimulus Generation

Stimuli were displayed on the screen of a Tektronix 690SR color monitor run at 120 interlaced frames/s. Stimuli were generated with an Adage 3000 raster-based frame buffer generator. 1024 output levels were specifiable for each gun. As many as 256 colors could be displayed on the screen in any frame. The color of an image was modulated sinusoidally in time by being cycled through a pre-computed color array. As many as 240 colors could be changed during the fly-back interval in a screen refresh. The 512×480 pixel display subtended an angle of

10.67×10 deg at the observer's eye. All stimulus presentation and data collection were done under automatic computer control.

Equation (6) was used iteratively to determine the amplitudes of Fourier descriptors of specified areas, numbers of lobes, and perimeter lengths. The plotting routine used a trapezoidal rule¹⁹ to integrate Eqs. (3) and (4) for the computation of the outer boundary. The boundary contour was filled in by a simple center-point expansion. The number of pixels constituting the Fourier shape was numerically counted as a check on the computed area. The resulting shape was then centered and run-length encoded to provide a compact and fast loading format for images.

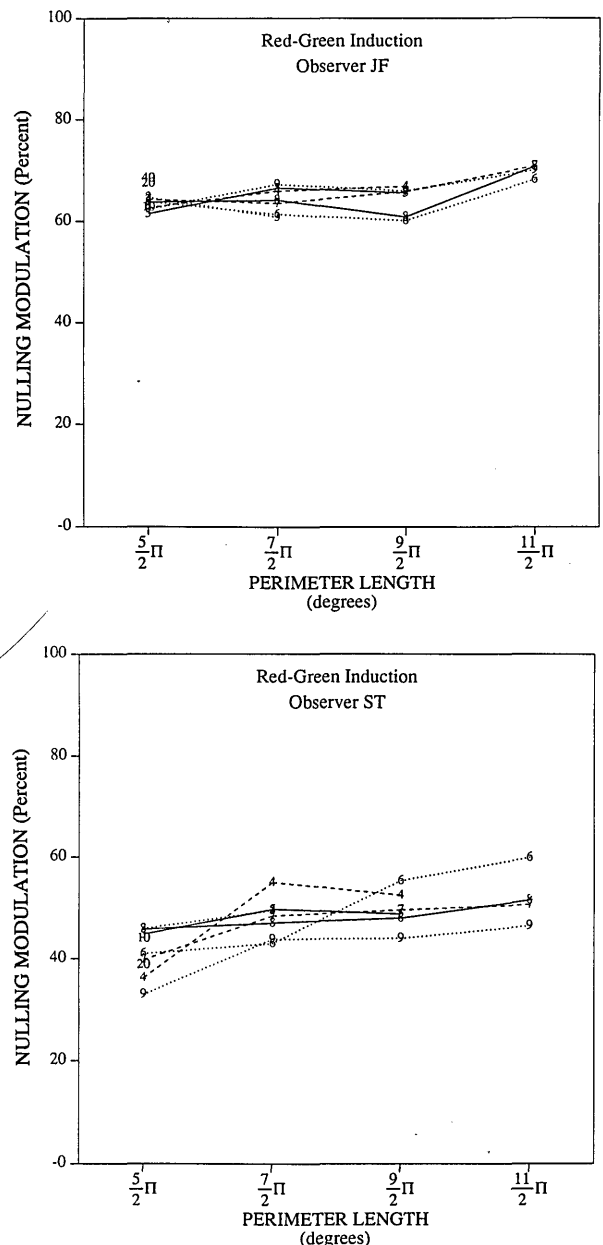


Fig. 5. Amplitude of nulling modulation in the red-green direction expressed as a percentage of inducing modulation versus the length of the perimeter of the test. Each test stimulus is represented by a number indicating the number of lobes that range from 3 to 40. Curves connect nulling amplitudes for tests of the same number of lobes.

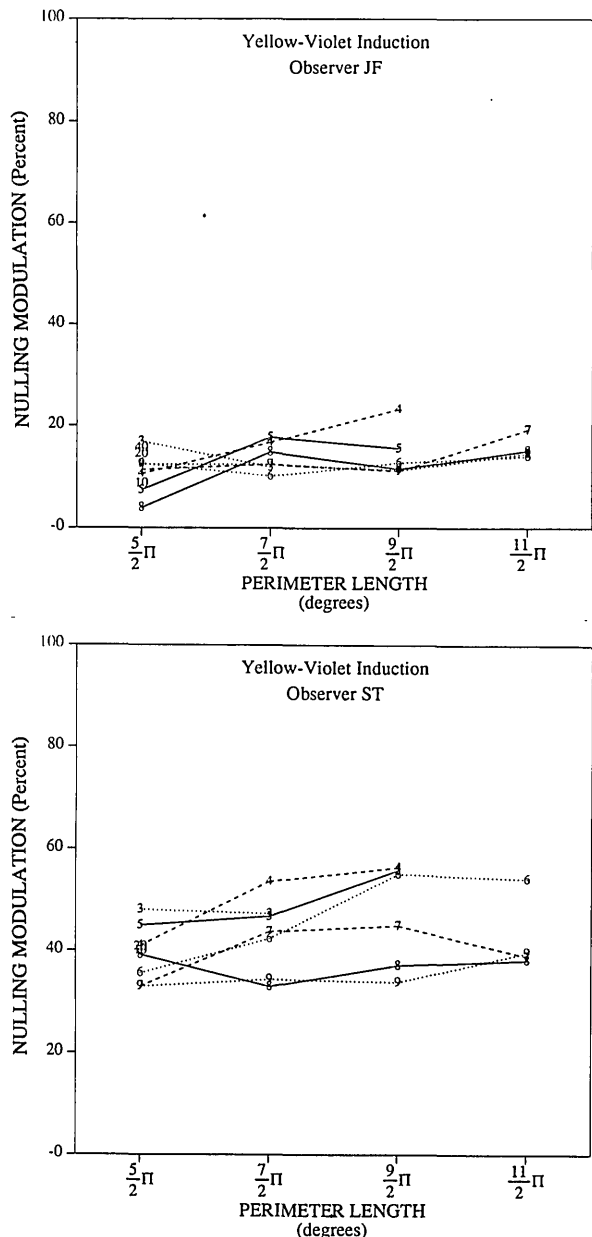


Fig. 6. Amplitude of nulling modulation in the yellow-violet direction expressed as a percentage of inducing modulation versus the length of the perimeter of the test. Each test stimulus is represented by a number indicating the number of lobes that range from 3 to 40. Curves connect nulling amplitudes for tests of the same number of lobes.

RESULTS

The results for light-dark, red-green, and yellow-violet induction are shown in Figs. 4, 5, and 6, respectively, for two color-normal observers. The amplitude of nulling modulation as a percent of the amplitude of inducing modulation is plotted on the vertical axis against the length of the perimeter for each Fourier test shape on the horizontal axis. Each data point is the mean of 30 observations and is shown as a number representing the number of lobes in the test shape. The results are simple: The magnitude of induced contrast does not depend on the length of the

perimeter of the test. In all six panels the slope of the best-fitting regression line was not significantly different from zero. The results have been replotted as the nulling modulation versus the number of lobes of the test shape in Figs. 7-9. The filled circles represent shapes of different perimeter lengths; the open squares represent the mean nulling modulation. The solid lines are the best-fitting regression lines. Again the results are simple: The hypothesis that the amount of induced contrast does not depend on the number of lobes of the test shape cannot be rejected. The regression lines have generally flat slopes. The best-fitting line in Fig. 9(b) has a negative slope; however, if the data for tests of 20 and 40 lobes were included [see Fig. 6(b)], the slope of the line would not be significantly different from zero.

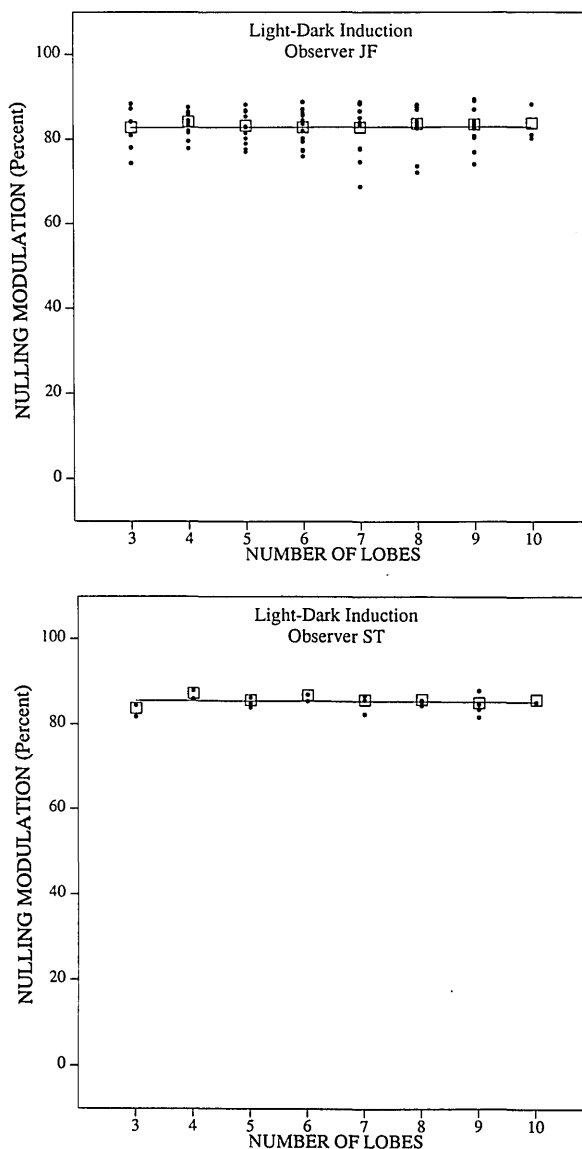


Fig. 7. Amplitude of nulling modulation in the light-dark direction expressed as a percentage of inducing modulation versus the number of lobes in the test. Filled circles represent repeated observations on tests of different perimeter length. Open squares represent the mean nulling amplitude for all tests of a particular number of lobes. The line is the best-fitting least-squares regression line.

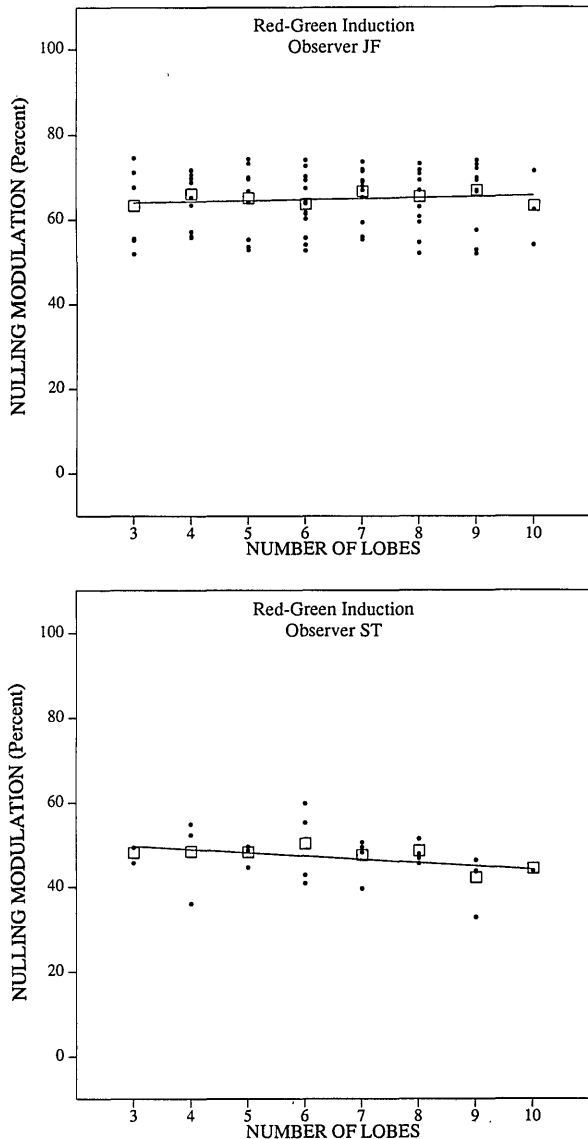


Fig. 8. Amplitude of nulling modulation in the red-green direction expressed as a percentage of inducing modulation versus the number of lobes in the test. Filled circles represent repeated observations on tests of different perimeter length. Open squares represent the mean nulling amplitude for all tests of a particular number of lobes. The line is the best-fitting least-squares regression line.

DISCUSSION

The results of the present experiment show that, for a spatially uniform central test and inducing surround, the magnitude of induced contrast is constant and does not depend on the shape or perimeter length of the test if the areas of the center and the surround are kept constant. Since this was a surprising result and since the test shapes in Fig. 1 vary considerably in narrowness of lobes, it was important to check that the amount of stray light from the surround was not significantly counteracting the induced effects. For the test shapes in Fig. 1, the amount of stray light from the surround falling inside the test was calculated from the light profile of the image of a point source for a 3-mm pupil tabulated by Vos *et al.*²⁰ The image consisting of the test Fourier shape and the surround

was divided into 1-min² pixels. For unit luminance, we calculated the fraction of light from each pixel of the surround that fell on the pixels inside the test. The fraction of the surround light falling inside the test, averaged over the number of test pixels, is expressed as a percentage in Table 1. The amount of space-averaged stray light is between 1% and 4% for all test shapes and is therefore not a significant contaminating factor in the results.

Psychophysical measurements have shown that the magnitude of induced contrast can be affected by parts of the visual field 2-3 deg from the center.²¹ Because information about long-range interactions between neurons is sparse,²² it is difficult to discuss color induction in terms of the properties of visual neurons. An attempt was made to relate the results of this study to elemental models for the computation of perceived color and brightness.

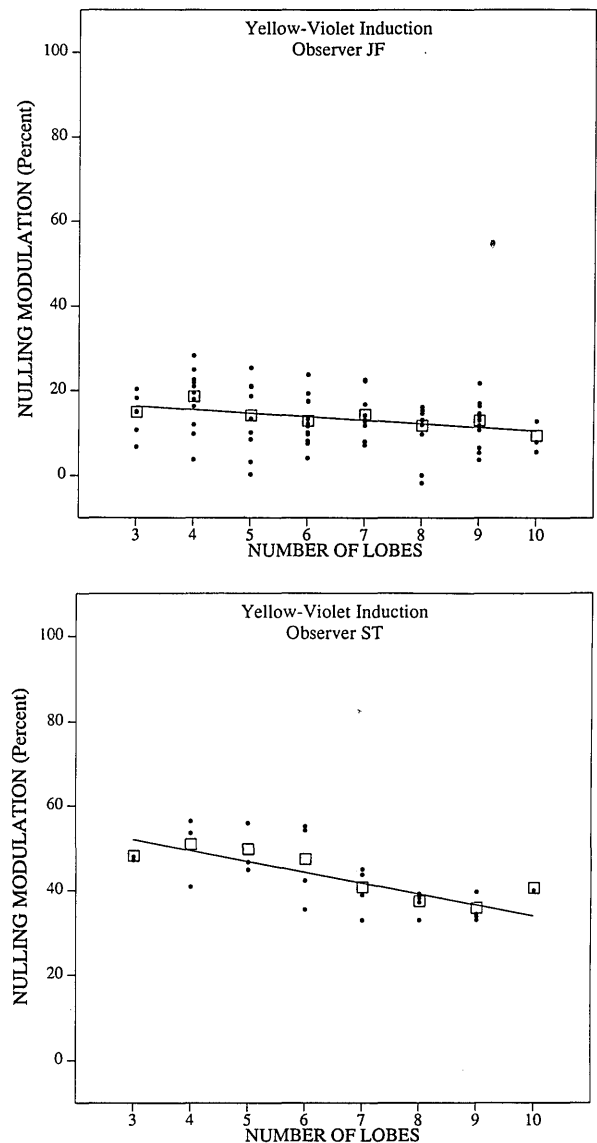


Fig. 9. Amplitude of nulling modulation in the yellow-violet direction expressed as a percentage of inducing modulation versus the number of lobes in the test. Filled circles represent repeated observations on tests of different perimeter length. Open squares represent the mean nulling amplitude for all tests of a particular number of lobes. The line is the best-fitting least-squares regression line.

Table 1. Space-Averaged Percentage of Stray Light Falling Within Test Region^a

Lobes	Perimeter Length			
	$\frac{1}{2}\Pi$	$\frac{3}{2}\Pi$	$\frac{5}{2}\Pi$	$\frac{7}{2}\Pi$
3	2.2	2.0	1.2	—
4	1.4	2.3	3.1	—
5	1.0	2.3	2.4	—
6	1.2	2.3	3.2	2.0
7	1.2	2.6	1.9	2.1
8	1.6	2.3	1.5	1.7
9	1.4	2.0	1.9	2.4

^aStray light was calculated from the light profile of the image of a point source for a 3-mm pupil tabulated by Vos et al.²⁰

The most developed of this class of models is the one by Grossberg and Todorović.⁸ This model uses elements that qualitatively mimic the spatial receptive field profiles of ganglion cells and V1 simple cells and sets up networks of interaction to create a contour-extracting stage followed by a filling-in stage. This model may embody some aspect of the underlying lateral interactions, but it has not been tested against quantitative data. In its present state of development it is not obvious how quantitative predictions could be generated. The final form of the model consists of a nonlinear diffusion equation for each point of a syncytium. At equilibrium this set of equations can be simplified to a set of simultaneous linear equations, but even then, because there is one equation per pixel, the solution requires inverting a massive matrix for a display of any realistic size. No simplifying assumptions are provided that could be used to modify the structure of the matrices so that the inversion can be made more efficient for special cases. The free parameters in the model are an additional problem. No scheme is provided for them to be estimated from empirical results or from any other considerations. Moreover, no sensitivity analysis of the model's equations has been presented, so it is not clear for what range of parameters the solution to the diffusion equations will converge in a reasonable fashion. A number of reasonable combination of parameters were tried without success and indicated the inaccessibility of the model to experimental testing.

Even though a mechanistic model is not achievable at present, models that link empirical results to physical properties of the stimuli could also prove useful as a guide to future research. The edge-distance [formula (1)] and the area-ratio [formula (2)] models of Yund and Armington¹¹ are two such physical models. In the present study the area of both test and surround was kept constant. The results showing approximately constant induced contrast are therefore consistent with, though not a critical test of, the area-ratio model. Formula (1) was derived for a disk-annulus configuration by Yund and Armington from a more general model.¹¹ To derive an expression for a Fourier shape from the more general model would require that one assume an arbitrary atheoretical function relating induced contrast to the angle between the edge and a radial line through the center. As an alternative, two different measures of proximity between the edge and elements inside the test were devised. The first measure was calculated from formula (7), where E was the distance from the center of the test to the edge along each

direction:

$$\sum_0^{2\pi} \frac{1}{E} \quad (7)$$

Since the surround was the same in all conditions, if induced contrast in the test were proportional to the proximity of the edge from the center, the measured nulling curves would have the form shown in Fig. 10. The horizontal axis shows the length of the perimeter, and the numbers in the curves refer to the number of lobes. The vertical axis shows predicted induced contrast in relative units. The relative magnitude of induced contrast pre-

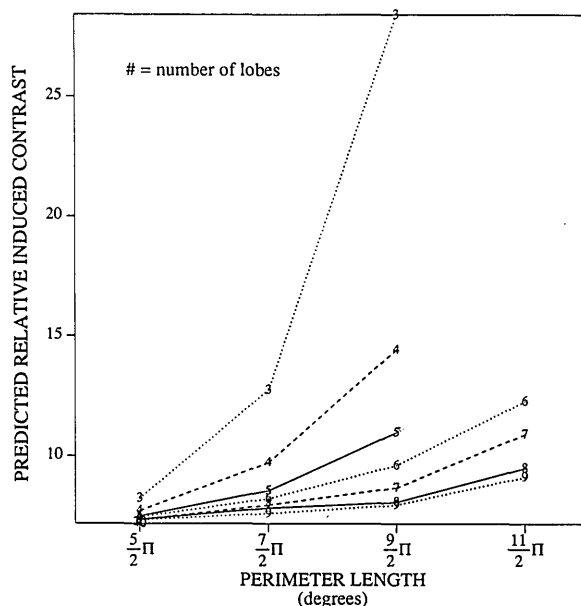


Fig. 10. Predicted induced contrast proportional to average $1/E$, where E is the distance from the center of the test to the edge along each angle.

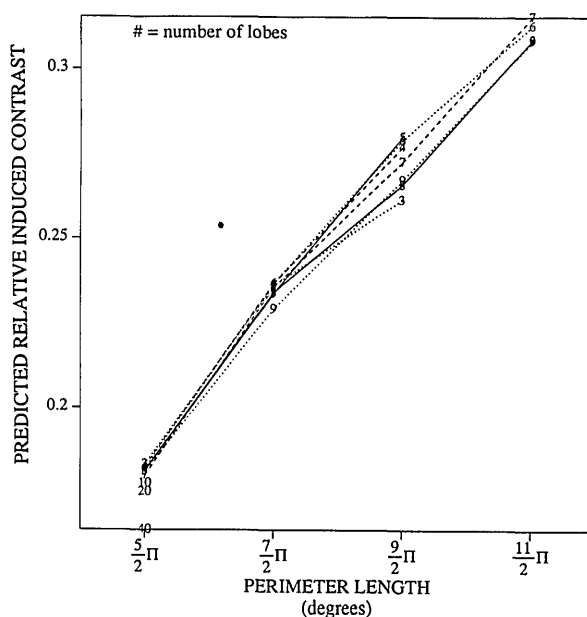


Fig. 11. Predicted induced contrast proportional to average $1/D$, where D is the distance from each test pixel to nearest surround pixel.

dicted by this model is an increasing function of perimeter length, especially for shapes with fewer lobes. The data in Figs. 4–6 are not consistent with this prediction. A second measure was calculated from formula (8), where D was the distance from each test element to the nearest surrounding element, and N the total number of elements in the test:

$$\sum \frac{1}{N D}. \quad (8)$$

The relative magnitudes of induced contrast predicted by this proximity measure are shown in Fig. 11 and again are not consistent with the data. It is probable that predictions from any edge-distance-based model will be dependent on the shape of the test and will therefore not be consistent with the data in Figs. 4–9.

In summary, for the spatial configurations tested in this study, the magnitude of induced contrast was constant when test and surround area were kept constant and did not depend on the shape or the length of the boundary between the test and the surround.²³ Combinations of the test shapes used in this study can be used to approximate a large variety of closed shapes.¹⁴ Consequently the results of this study probably hold true for tests of almost any shape. The three color directions used in this study were chosen to be representative of color space. Krauskopf et al.⁵ showed that induction along an arbitrary color line cannot be predicted by the magnitude of induction along the cardinal or any other threesome of color axes. However, because the results are similar for each of the three cardinal axes, it is likely that the results of this study are correct for all color directions.

ACKNOWLEDGMENTS

This research was partially supported by National Institutes of Health grant EY07556 to Q. Zaidi. Comments by Ben Sachtler and Steve Shevell on an earlier version of this manuscript are gratefully acknowledged.

REFERENCES AND NOTES

1. E. Mach, *The Analysis of Sensation and the Relation of the Physical to the Psychological* (Open Court, Chicago, 1914).
2. E. H. Adelson, "Lightness judgements and perceptual organization," *Invest. Ophthalmol. Vis. Sci. Suppl.* **31**, 265 (1990).
3. A. L. Gilchrist, "When does perceived lightness depend on perceived spatial arrangement?" *Percept. Psychophys.* **28**, 527–538 (1980).
4. M. E. Chevreul, *The Principles of Harmony and Contrast of Colors* (Van Nostrand Reinhold, New York, 1848).
5. J. Krauskopf, Q. Zaidi, and M. B. Mandler, "Mechanisms of simultaneous color induction," *J. Opt. Soc. Am. A* **3**, 1752–1757 (1986).
6. G. S. Brindley, *Physiology of the Retina and Visual Pathway* (Williams and Wilkins, Baltimore, Md., 1960).
7. A. M. Marsden, "An elemental theory of induction," *Vision Res.* **9**, 653–663 (1969).
8. S. Grossberg and D. Todorović, "Neural dynamics of 1-D and 2-D brightness perception: a unified model of classical and recent phenomena," in *Neural Networks and Natural Intelligence*, S. Grossberg, ed. (MIT, Cambridge, Mass., 1988), pp. 127–194.
9. L. E. Arend and R. Goldstein, "Lightness modes, gradient illusions, and curl," *Percept. Psychophys.* **42**, 65–80 (1987).
10. A. Blake, "Boundary conditions for lightness computation in Mondrian world," *Comput. Vision Graphics Image Process.* **14**, 314–327 (1985).
11. E. W. Yund and J. C. Armington, "Color and brightness contrast effects as a function of spatial variables," *Vision Res.* **15**, 917–929 (1975).
12. H. Helson, *Adaptation-Level Theory* (Harper & Row, New York, 1964).
13. D. J. Heeger, "Nonlinear model of neural responses in cat visual cortex," in *Computational Models of Visual Processing*, M. Landy and A. Movshon, eds. (MIT, Cambridge, Mass., 1991), pp. 119–133.
14. C. T. Zahn and R. Z. Roskies, "Fourier descriptors for plane closed curves," *IEEE Trans. Comput.* **C-21**, 269–281 (1972).
15. T. M. Apostol, *Mathematical Analysis*, 2nd ed. (Addison-Wesley, Reading, Mass., 1974).
16. J. Krauskopf, D. R. Williams, and D. H. Heely, "The cardinal directions of color space," *Vision Res.* **22**, 1123–1131 (1982).
17. D. I. A. MacLeod and R. M. Boynton, "Chromaticity diagram showing cone excitation by stimuli of equal luminance," *J. Opt. Soc. Am.* **69**, 1183–1186 (1979).
18. V. C. Smith and J. Pokorny, "Spectral sensitivity of the foveal cone photopigments between 400 and 700 nm," *Vision Res.* **15**, 161–171 (1975).
19. W. H. Press, B. P. Flannery, S. A. Teukolsky, and W. T. Vetterling, *Numerical Recipes in C* (Cambridge U. Press, New York, 1987).
20. J. J. Vos, J. Walraven, and A. van Meeteren, "Light profiles of a foveal image of a point source," *Vision Res.* **16**, 215–219 (1976).
21. Q. Zaidi, B. Yoshimi, and N. Flanigan, "Test of spatial additivity for induced color contrast," in *Optical Society of America Annual Meeting*, Vol. 15 of 1990 OSA Technical Digest Series (Optical Society of America, Washington, D.C., 1990), p. 206.
22. D. Y. Tso and C. D. Gilbert, "The organization of chromatic and spatial interactions in the primate striate cortex," *J. Neurosci.* **8**, 1712–1727 (1988).
23. A referee has asked whether the results in this study would hold for perceived induced contrast if measured by a matching method. The answer is in the affirmative if roughly equal nulling amplitudes correspond to roughly equal matching amplitudes. This will be the case if the two are related by any reasonably smooth function. The nulling method, however, has many advantages over matching methods. Major drawbacks of matching and memory methods were explained by H. Helmholtz, *Physiological Optics* (Optical Society of America, Washington, D.C., 1924), Vol. 2, pp. 264–271.